# Development of a frugal, in-situ sensor implementing a ratiometric method for continuous monitoring of turbidity in natural waters

Raul Sanchez, Michel Groc, Renaud Vuillemin, Mireille Pujo-Pay, Vincent Raimbault

# Development of a frugal, in-situ sensor implementing a ratiometric method for continuous monitoring of turbidity in natural waters

**Raul Sanchez [1], Michel Groc[2], Renaud Vuillemin[2], Mireille Pujo-Pay[3] and Vincent Raimbault [1,*]**

[1] LAAS-CNRS, Université de Toulouse, CNRS, Toulouse, France;

[2] Sorbonne Université, CNRS, FR3724, Observatoire Océanologique de Banyuls, Paris, France;

[3] Sorbonne Université, CNRS, UMR7621, Laboratoire d'Océanographie Microbienne (LOMIC), Paris, France;

* Correspondence: vraimbau@laas.fr;

**Abstract:** Turbidity is a commonly used indicator of water quality in continental and marine waters, mostly caused by suspended and colloidal particles such as organic and inorganic particles. Many methods are available for the measurement of turbidity, ranging from the Secchi disk to infrared light-based benchtop or in-situ turbidimeters as well as acoustic methods. The operational methodologies of the large majority of turbidity instruments involve the physics of light scattering and absorption by suspended particles when light is passed through a sample. As such, in the case of in-situ monitoring in water bodies, the measurement of turbidity is highly influenced by external light and biofouling. Our motivation for this project is to propose an open-source, low-cost in-situ turbidity sensor with a suitable sensitivity and operating range to operate in low to medium turbid natural waters. This prototype device combines two angular photodetectors and two infrared light sources with different positions, resulting in two different types of light detection: nephelometric (i.e. scattering) and attenuation light, according to the ISO 7027 method. The mechanical design involves 3D-printed parts by stereolithography which are compatible with commercially available waterproof enclosures, thus ensuring easy integration for future users. An effort has been made to rely on mostly off-the-shelf electronic components to encourage replication of the system, with the use of a highly integrated photometric front-end commonly used in portable photoplethysmography systems. The sensor was tested in laboratory conditions against a commercial benchtop turbidimeter with Formazin standards. The monitoring results were analysed getting a linear trendline from 0 to 50 Nephelometric Turbidity Unit (NTU), and an accuracy of +/- 0.4 NTU in the 0 to 10 NTU range with a response time of less than 100 ms.

**Keywords:** Turbidity; Frugal sensors; Ratiometric; in-situ; Water quality

## 1. Introduction

Turbidity is an important indicator of water quality in rivers, streams, lakes, sea and watershed, and as such a key parameter for environmental studies as well as for the health of human intake [1]. It is basically a physical property of fluids that measure of the cloudiness of water, and is influenced by the presence of suspended and dissolved particles that blocks or scatter the light in water bodies, thus modifying water transparency [2]. These particles can be of organic or inorganic origin. In the case of organic materials high turbidity can indicate presence of microorganisms like bacterias or events like algae blooms. In the case of inorganic materials high turbidity can indicate high suspended sediments like clay or silt, caused by erosion [3,4]. Besides human interference, the environment's turbidity level can be influenced by nutrient run-off or soil erosion from farming [5], but also by geological disturbances that can cause turbidity currents [6,7].

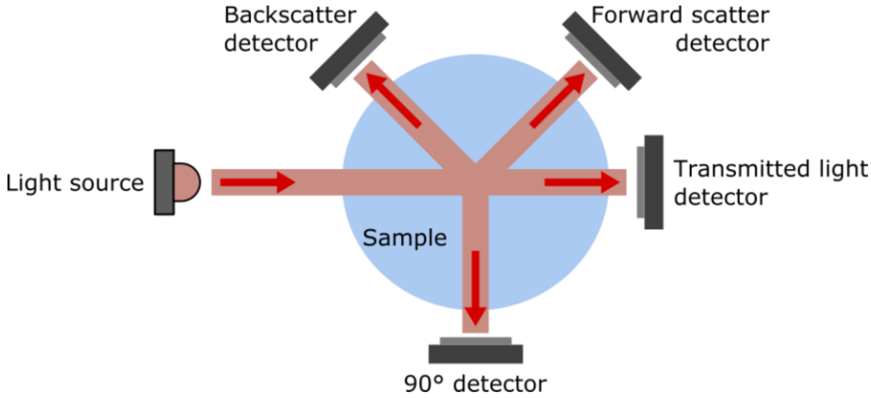


*Figure 1. Illustration of the most common optical configurations adopted in turbidity measurement devices.*

Commercial turbidity systems are mostly offline systems, that requires the action of a trained operator to collect the samples and perform the analysis either on site (portable system), or in a laboratory (benchtop system). While this approach offers generally the most precise turbidity measurements, it limits the spatial and temporal resolution. This punctual water sampling also does not allow to observe sudden events, and atop of the equipment cost adds up operational costs (human resources, travel, sample storage …). In some cases, it is thus highly desirable to use in-situ turbidity sensors; while commercial in-situ turbidity sensors are readily available, their adoption is limited by their high cost (several thousands of US dollars typ.) that also limits spatial and temporal resolution. While the need for a low-cost, in-situ turbidity sensor has been already explored in the literature, our goal is to backup these efforts with a sensor that can be used in low turbidity areas like the French coastal area of the Mediterranean Sea, as well as in more turbid freshwater systems.

*Turbidity measurement methods*

While complementary methods like acoustic [8] or time resolved [9] are also used for specific cases, turbidity is mostly measured optically by a combination of a light source and one or more photodetectors that measure the scattering and/or absorption properties of particles suspended in the water sample. While absorption is a directional measurement, scattering occurs in all directions, with a diffraction pattern dependent on the particle size [10], hence different optical configurations can be implemented. The most common configurations are represented Figure 1. Depending on the angle between the light source and the detector, they are referred as nephelometric (angle = 90°), attenuation (angle = 180°), backscattering (0° < angle < 90°) or forward scattering (90° < angle < 180°). Based on the angle used for the measurements, different type of units are used, the most common being Nephelometric Turbidity Unit (NTU), but others units like Formazin Nephelometric Unit (FNU) or Formazin Attenuation Unit (FAU) can be encountered [4].

Each configuration will behave differently regarding turbidity. Backscattering is considered to be suitable to high turbidity values only (> 1000 NTU), and as such is not of direct interest in our work. Nephelometric (90° detection angle) is considered the best angle to measure scattered light regardless of particles size [11], but is advised to be used between 0 to 40 NTU, where light intensity and turbidity have a linear relationship [12]. Attenuation (180° detection angle) measure the transmitted light through the sample and is affected by combined effects of scattering and absorption: an increase in turbidity translates to a decrease of transmitted light. Attenuation method is only recommended for turbidity levels over 40 NTU [5,13], however it is also used as a secondary detector in combination with a 90° detector in ratiometric designs. Turbidity measurements are normalized by internationally recognized certification organisms. The main approved turbidity methods are ISO 7027-1 and US-EPA Method 180.1, but other methods like Standard Methods 2130B and Great Lakes Instrument Method 2 (GLI Method 2) are also endorsed by the US-EPA [13–16]. A good overview of the different configurations used in each method can be obtained in references [17,18].

*Turbidity sensors calibration*

Due to the diversity of turbidity sources, the calibration of turbidimeters using natural sediment sources is problematic in most cases, especially for intercomparing between different instruments. To obtain a more standardized, repeatable calibration method, a polymer called Formazin [19] has been adopted by most of the manufacturers in the industry. It is prepared by mixing solutions of hydrazine sulfate and hexamethylenetetramine in water [20] to obtain different chain lengths in random configurations, covering a range of particle shapes and sizes from less than 0.1 to over 10 microns, making it a relatively straightforward light-scattering calibration standard. One of its main advantages is that it can be repeatably and reproducibly prepared from raw materials into a calibrated stock solution that is diluted to obtain virtually any concentration. Under proper storage conditions, Formazin standards is stable over a year, apart from very low concentrations (< 2 NTU) where long-term stability is degraded.

Although being the calibration standard of choice of the most common official turbidity measurement methods, Formazin has also a couple of inherent drawbacks which have been summed up in Kitchener et al. work [21]. In particular, the shape of Formazin particles is not normalized, although particles shapes can have strong influence on side-scattering. Is should also be stated that uncertainties arose due to the high dilution ratios typically required at low turbidity, reinforced by the lack of stability of these highly diluted solutions. It is commonly observed that when used with the same Formazin calibration solution, commercial turbidimeters that fulfil requirements of the same official standard (EPA/ISO) can give different turbidity values. This has been observed on laboratory benchtop instruments, but also for in-situ instruments [22,23]. Research on better calibration methods of existing turbidimeters, as well as design of new instruments that overcomes the lack of comparability between current instruments [24] are out of the scope of this present work, but some design recommendations have been incorporated in our sensor as suggested by other authors.

*Commercial and research-level instruments*

As a ubiquitous water quality parameter, a lot of commercial instruments are available to measure turbidity. The vast majority is based on optical measurement in the infrared using side-scattering, back-scattering, attenuation or a combination of these in order to satisfy the officially endorsed methods described earlier. The instruments can be classified within three categories: (i) benchtop instruments, which offers the best accuracy, (ii) hand-held portable devices, which are the least expensive options, (iii) inline sensors which are dedicated to analysis in water pipes and (iv) in-situ sensors which can be “self-contained” or available as an add-on for multiparameter sondes. Both (i) and (ii) requires to sample the water bodies for further analysis, and as such are not adapted for real-time monitoring, remote monitoring, or high spatio-temporal resolution measurements as they would require an impractical amount of work for sampling, storage and analysis.

Pricewise, a commercial turbidimeter cost between 600 to more than 5000 USD, portable hand-held devices being the most affordable option, while high-precision benchtop instruments tend to be the most expensive. In-situ sensors, which are the scope of this paper, are usually in the middle of the range, but most of the time they need additional equipment like a logger or a display for example, which makes a complete setup costing several hundreds of USD. Due to the constraints of in-situ measurements of water bodies, which include instrument damages due to natural phenomenon, robbery, degradation by humans or wildlife, and the necessity in some cases to collect data at a better spatio-temporal resolution, the relatively high cost of commercial instruments has led to a lot of research on alternative, low-cost turbidity sensors, that while compromising slightly on measurement quality, can provide valuable data at a fraction of the cost. Table 1 lists recent achievements reported in the literature. A comprehensive list of commercially available turbidimeters can be found in the Aquaref report [25] as well as in the inter-comparison study of Rymszewicz et al. [22] that focuses on in-situ instruments.

**Table 1.** Recent achievements in the literature on turbidimeter developments.

| Sensor | Range | Resolution | In-situ | Method | Reference |
|---|---|---|---|---|---|
| Fay et al. | 0-100 NTU<br>0-1000 NTU | | No | ISO 7027 | [26] |
| Kitchener et al. | N.A. | | No | TARDIIS | [24] |
| Gillett et al. | 0-100 NTU | 1 NTU | No (continuous) | Nephelometry | [27] |
| Trevathan et al. | 100-400 NTU | | Yes | Attenuation | [28] |
| Zang et al. | 40-300 NTU | 3 NTU | No | Nephelometry and attenuation | [29] |
| Matos et al. | 0-4000 NTU | N.A. | Yes | IR backscatter, nephelometry and attenuation | [10] |
| Metzger et al. | 0.1-1000 NTU | 0.04 to 3 NTU | No | ISO 7027 | [30] |
| Parra et al. | 0-200 NTU | N.A. | No | Attenuation | [31] |
| Kelley et al. | 0-1000 NTU | 0.02 NTU | No | Nephelometry | [32] |
| Our work | 0-100 NTU | 0.4 NTU | Yes | GLI2 | N.A. |

## 2. Materials and Methods

The development of our in-situ turbidity sensor is targeted toward coastal waters at the Oceanological Observatory of Banyuls sur Mer (OOB), France. In this area of the Gulf of Lion in the Mediterranean Sea, turbidity levels are considered quite low with average values ranging from 0 to 10 NTU typically during the year, which implies that the sensor must offer sufficient resolution (i.e. 0.5 NTU or better). Biofouling is also a common occurrence during long-term deployment of optical sensors in this area, as observed at the OOB as a part of the French Coastal Monitoring Network SOMLIT.

Based on these constraints, we choose to design our sensor around the Great Lakes Instruments Method 2 (GLI 2), also referred as modulated four-beam turbidimeter, which uses two light sources (infrared LEDs) and two photodetectors (photodiodes) to perform a ratiometric measurement that combines nephelometric and attenuation readings. This method improves instruments stability, by cancelling out errors due to the degradation of the light source, water color effects or fouling on the sensor windows [21]. Even if all four optical ports are partially blocked, this method can still provide accurate turbidity measurements [33]. The LEDs alternate light pulses periodically and the two photodetectors takes simultaneous readings, providing an active signal and reference signal. This operating principle is summarized Figure 2. Operating range is typically 0-100 NTU, however it loses some accuracy in levels above 40 NTU. GLI 2 is known to be very accurate for lower turbidity ranges, in particular within the 0-1 NTU range [16], which makes this type of instrument desirable for water bodies with low turbidity. The capability to limit the influence of light source drift and fouling also are a plus when considering in-situ deployment. However, the design layout makes this method harder to integrate into a field deployable instrument, compared to a conventional nephelometer where both the light source and the photodetector can be protected by a flat optical surface. Another advantage of the GLI 2 design is the ability to get information on side-scattered light (nephelometric) and attenuation (transmission); the latter being recommended to be include in new turbidity instrumentation by Kitchener et al. [21], as it allows for the use of SI based units for calibration. Compared to conventional nephelometric instruments which are calibrated with Formazin, this allows better intercomparison to other turbidimeter, a characteristic that is currently lacking from commercial systems as highlighted by Rymszewicz et al. [22]. To our knowledge, our sensor is the first academic work on a GLI 2 based design that can operate continuously in-situ.

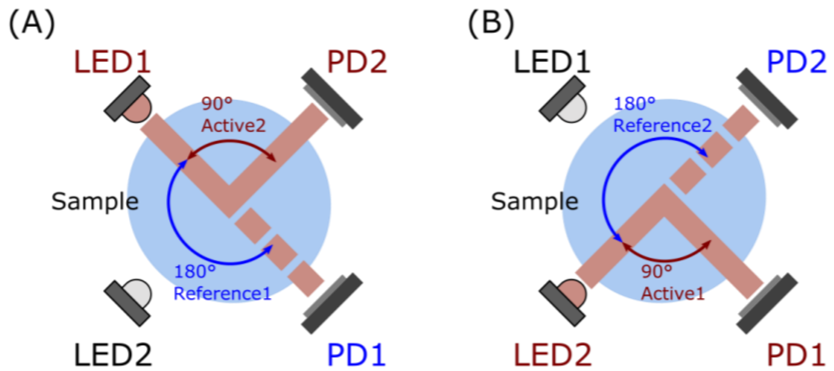


*Figure 2. Illustration of the GLI-2 method, a ratiometric method based on a modulated 4-beam design. (A) Phase one, light source LED1 is on, photodetector PD2 measures the Active2 signal (90° nephelometric) and photodetector PD1 the Reference1 signal (180° attenuation). (B) Phase two, light source LED2 is on, photodetector PD2 is the Reference2 signal (180° attenuation) and photodetector PD1 is the Active1 signal (90° nephelometric).*

### *2.1. Overview of the turbidity sensor*

Our turbidity sensor, referred as OpenProbe GLI 2, possesses two infrared LEDs and two infrared photodiodes in order to implement the GLI 2 method. For the infrared LEDs we use the OSRAM SFH 4718A that has its peak wavelength at 860 nm, a Full Width at Half Maximum (FWHM) of 34 nm, and supports up to 1000 mA of forward current. For photodetectors, we use the OSRAM SFH 2700 FA A01, a silicon PIN photodiode with a daylight blocking filter that translate to a spectral sensitivity from 700 to 1100 nm.

The main functions required to use these optoelectronics components are LED drivers, transimpedance amplifiers, and an Analog to Digital Converter (ADC). Absorption underwater is stronger for longer wavelengths, so the use of IR photodiodes limits the influence of daylight during in-situ measurements. However due to the relatively small variations caused by turbidity, an ambient light rejection strategy is still required, and is taken care of by synchronous detection. While each of these functions can be achieved by discrete components, we choose to design our system around the ADPD1080 from Analog Devices, a highly integrated photometric front-end initially designed for photoplethysmography (PPG) in wearables or smartwatches, as it includes all the required features in a single low-power Integrated Circuit (IC), which is highly beneficial in terms of cost, miniaturization, and power consumption. Is possesses three LEDs drivers with up to 370mA current capability, the possibility to connect up to 8 photodetectors to its transimpedance amplifier (TIA) with digitally adjustable gains, and has an Analog Front-End (AFE) which is in charge of the rejection of signal offset and corruption due to the interference caused by ambient light, and has a 14-Bit ADC.

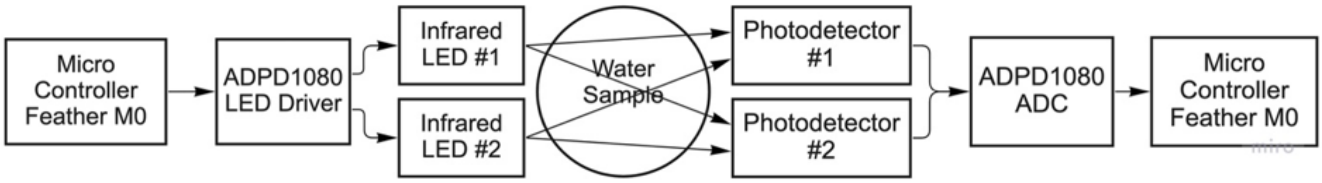


*Figure 3. Block diagram of the OpenProbe GLI 2 sensor.*

The block diagram on Figure 3 describes the overall architecture of the turbidimeter. An Adafruit Feather M0 microcontroller is used to control the different components, as it is a popular open-hardware configuration for environmental sensor projects [34,35]. Based around a low-power ATSAMD21G18 ARM cortex M0 processor, clocked at 48 MHz and 3.3V logic, it can work with any 3.7V Lithium polymer battery as power supply, and integrates a charge circuitry. This microcontroller is available in different versions with wireless communication capabilities (BLE, LoRa, WiFi) with the same form-factor, which allows to select the most appropriate communication standard based on the user needs. Depending on our needs, we used either the RFM95 LoRa version, which allows long-range wireless transmission of turbidity data, or the Bluefruit LE version (nRF51822 chipset for Bluetooth Low Energy communications) that allows easy short-distance communication with a smartphone or a laptop for example. Functionalities can easily be added in the form of add-on boards: for the data acquisition we use the Adafruit Adalogger FeatherWing which integrates a PCF8523 real time clock and a microSD memory card socket to handle datalogging functions, i.e. timestamping and data recording as text files. The microcontroller controls the ADPD1080 photometric front-end through an I2C interface, in order to adjust the various settings for LED drivers, TIA gain and various timings.

### *2.2. Hardware design*

To achieve the communication between the ADPD1080 photometric front-end and the Adafruit Feather M0 microcontroller, additional components are required. An AP7313 low dropout voltage regulator is used to supply a clean 1.8V voltage to the ADPD1080 from the Adafruit Feather M0 3.3V output regulator. A PCA9306 I2C bus voltage-level translator is used between the 3.3V logic level of the microcontroller and the 1.8V logic level of the photometric front-end for the SDA and SCL lines, with 2.2 kohms pull-up resistors. Finally, an ADG3304 bidirectional logic level translator is used for the GPIO0 and GPIO1 pins which are used for generating hardware interrupts on the microcontroller when data is available.

Optoelectronics components, i.e. LEDs and photodiodes, are integrated on a separate PCB to ensure proper positioning and implement the GLI 2 method. Due to the use of SMD components, the spatial distribution required, and the need of integration in a waterproof enclosure for in-situ measurements, we chose to design a custom flexible PCB that is bent in a circular shape to obtain proper positioning of the optical elements, as illustrated Figure 4 (A). Both PCBs are connected through Molex Picoblade 6 pins cable and connectors. The two-layer and the flexible PCBs are manufactured by the OSH Park company, and the components are assembled in-house using a reflow oven. The complete circuit diagram, CAD files and pictures of the electronics are available in the repository given in Supplementary Material section (https://gitlab.laas.fr/vraimbau/OpenProbe).

### *2.3. Sensor Housing*

The literature is scarce on GLI-2 ratio-based instruments for in-situ turbidity measurement; based on the recent achievements presented in Table 1, we attribute this to the apparent complexity of building a waterproof enclosure for this four-beam design with equipment available in an academic facility. In order to make our design easily replicable, we tried to develop our sensor around off-the-shelf components and standard equipments/techniques that can be either outsourced or purchased. The waterproof enclosure is made by stereolithography (SLA) with a desktop Formlabs Form 3 3D printer and Black Resin, a methacrylate-based material. After development in isopropanol (Formlabs Form Wash), parts undergo are cured overnight at 60°C. This unusually long curing step is required for the subsequent overmolding step with polydimethylsiloxane (PDMS), as it has been observed that commercially available SLA resins inhibits its polymerization without this treatment [36]. The flexible PCB with its mounted LEDs and photodiodes is bent to be inserted within the enclosure, with mechanical features that guides the LEDs and photodiodes to ensure proper alignment (Figure 4 (A)).

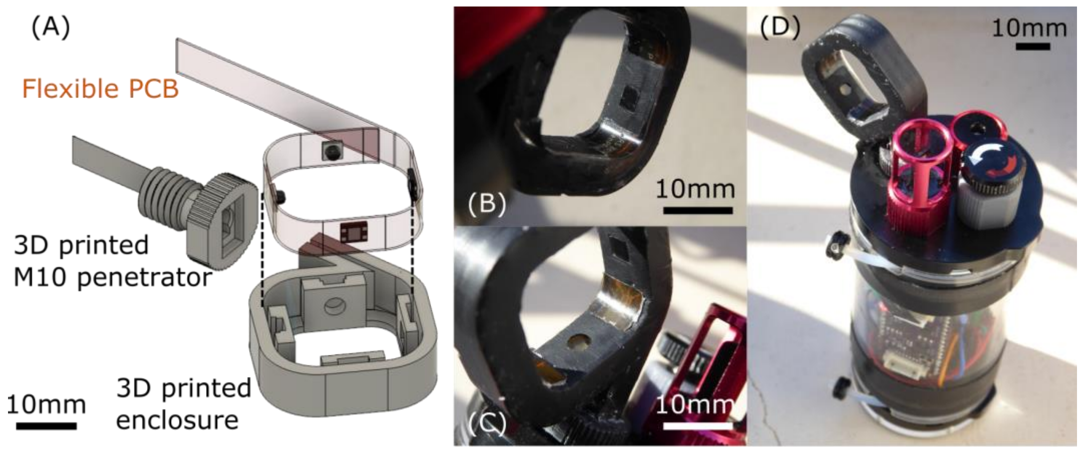


*Figure 4. (A) CAD illustration of the GLI-2 sensor, with the flexible PCB hosting the two IR LEDs and the two photodiodes, the 3D printed enclosure and a 3D printed M10 penetrator that makes the sensor compatible with Blue Robotics waterproof enclosures. (B) and (C) Close-up pictures of a photodiode and a LED optical port respectively, after the PMDS overmolding step, to illustrate the good transparency and optical properties obtained with our method. (D) Implementation for in-situ deployment, with the electronics and LiPo battery protected behind a Blue Robotics 2-inch diameter enclosure, showing the GLi-2 sensor head as well as additional pressure (depth) and temperature sensors.*

We then use overmolding with PDMS (Sylgard 184 – Dow Corning) to ensure waterproofness and optical transparency for the optical elements. This also ensures that no air is trapped in the housing, which is a key factor to obtain a sensor that can be used at depth in the water column. A 1:10 ratio PDMS mixture is poured over the 3D printed enclosure and the flexible PCB, with the help of a 3D printed insert covered with a Kapton film in the centre to create a smooth, yet anti-sticking interface at each optical port. The whole assembly is polymerized at 65°C overnight, and then the insert with the Kapton film is removed, leaving optically clear and smooth windows in front of each optical elements, as visible in Figure 4 (B) and (C) closeup views. In order to facilitate sensor testing and further replication, we designed and printed a M10 penetrator adapter to make our turbidity sensor compatible with the Blue Robotics waterproof enclosures that are regularly used in environmental sensor development [37]. We used a 2-inch diameter, 100mm long cast acrylic tube which is rated for 300 m depth, which houses the Adafruit Feather M0, the Adafruit Adalogger FeatherWing, our custom ADPD1080 PCB and a LiPo battery, as well as additional sensors, in this case pressure (depth) and temperature.

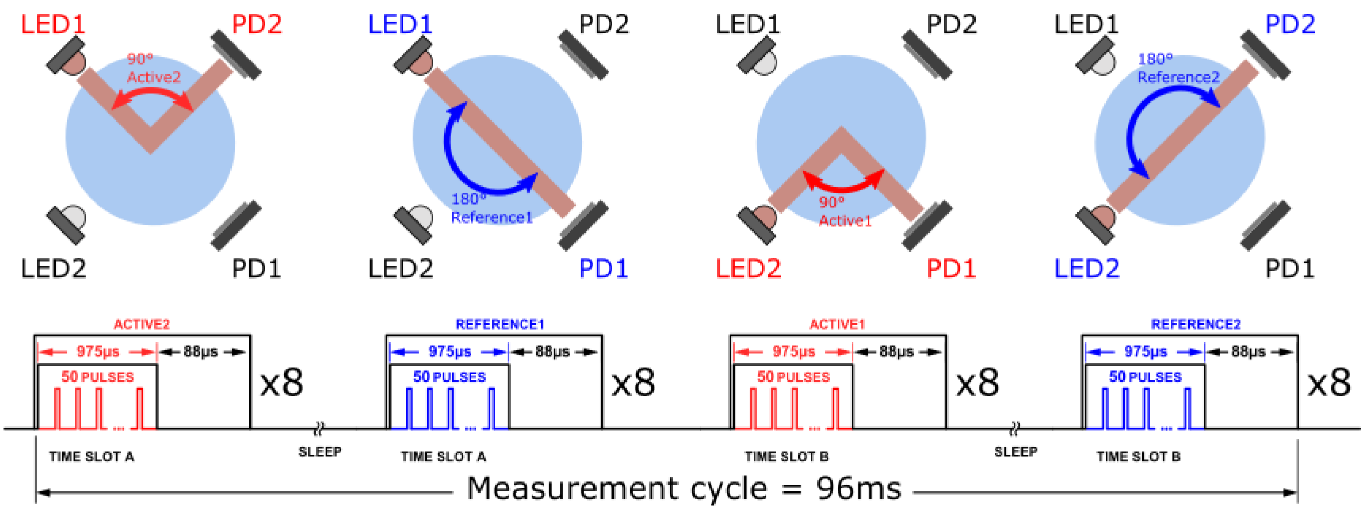


*Figure 5. Measurement sequence implemented by the software to measure Active2, Reference1, Active1 and Reference2 signals and corresponding timing diagram illustrating the AFE operation. Each step is performed 8 times to perform internal averaging which allows to improve signal to noise ratio. Total measurement time in this configuration is 96 ms.*

### *2.4. Software*

The Adafruit Feather M0 is programmed through the Arduino IDE environment, with a custom library to handle the specific functionalities of the ADPD1080. The operation principle of the photometric front-end consists in the stimulation of the LEDs during short pulses (in our case, 3µs duration) and the synchronous measurement of the returning signal from the photodetectors through the analog block. An integrator allows to sum up the returning signal from an adjustable number of pulses, allowing for an increase in the Signal to Noise Ratio. The ADC output is obtained by the microcontroller either through the use of hardware interrupts (using GPIO0 and GPIO1 pins of the ADPD1080), which are generated each time new data is available in the ADC output register, or by data polling at regular interval. While data polling is easier to implement, the use of hardware interrupt is more robust and allows for better efficiency of the code, especially if one consider optimizing the battery life of the system. To operate the GLI 2 method, four steps are required, as described Figure 5 which represent the measurement sequence, as well as the timing diagrams. Settings of the photometric front-end for each measurement step have been optimised. Pulse number per step is 50, the

TIA gain is set to 50kΩ, and LED current is set to 260mA for Active measurement (nephelometric) and 70mA for Reference measurement (attenuation). The AFE possess an internal averaging function that allows to lower the noise, to the expense of a longer response time and higher power consumption. We set the averaging factor to 8, which using the optimised settings lead to a response time of about 100 milliseconds for a complete measurement cycle. As a comparison, our handheld AQ3010 device takes approximately 20 seconds to deliver a measurement. This very short response time is particularly valuable to measure turbidity profiles, i.e. variation of turbidity versus depth. Increasing the averaging factor above 8 only resulted in relatively small improvement on the noise level.

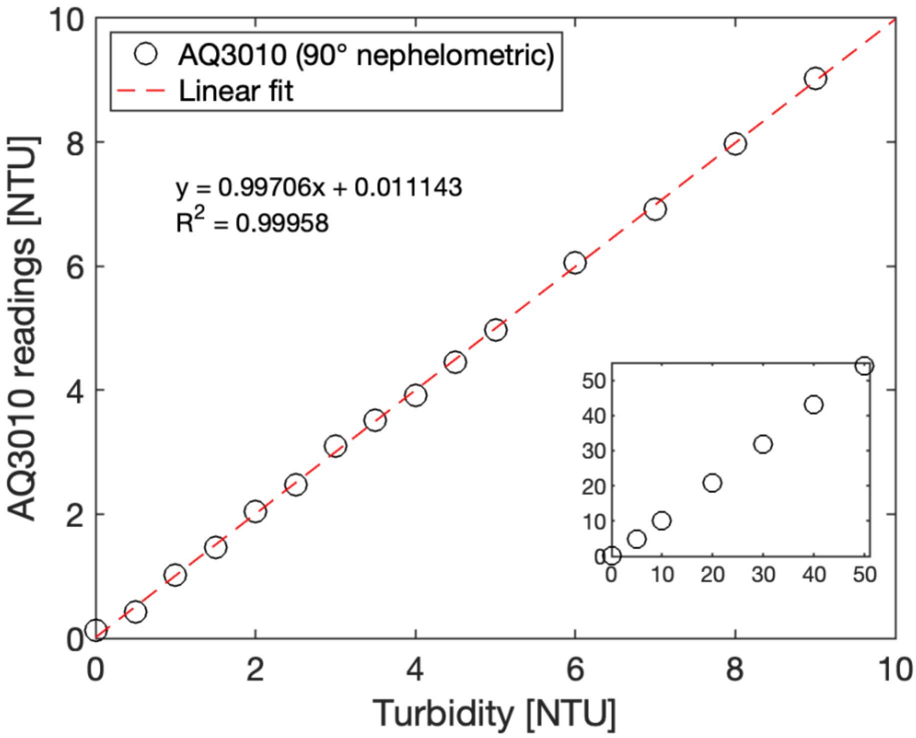


*Figure 6. Graph of a calibrated Thermo Scientific Aquafast AQ3010 Turbidity meter to Formazin solutions from 0 to 10 NTU (main graph) and 0 to 50 NTU (inset).*

## *2.5. Formazin standard calibration method*

While the calibration of turbidimeters with Formazin suffers from limitations as mentioned in the introduction section, this calibration method is the current standard of reference methods, and as such is selected in this work. Turbidity calibration solutions are made by dilution of a 4000 NTU Formazin Turbidity Standard (Hach) in laboratory grade deionized water. Solutions are prepared daily to avoid stability issues, and are remixed prior to measurements to avoid suspension to settle out. Solutions are then measured using our reference instrument, a commercial Thermo Scientific Aquafast AQ3010 Turbidity Meter which is a handheld device that uses 90° nephelometric method and outputs turbidity in NTU units. Figure 6 summarize the data obtained with this instrument for 0 to 50 NTU solutions. The increments between each solution have been adapted to the turbidity levels, with 0.5 NTU increments in the low range, and 10 NTU increments in the high range. The 0 NTU blank solution is the same laboratory grade deionized water used for dilutions of the 4000 NTU Formazin standard.

## 3. Results

### *3.1. Photodetector current*

The ADPD1080 photometric front-end is a complex component with many different settings that can influence drastically its performance. Prior to its use, we choose to validate the behaviour of our optoelectronic component selection and enclosure design through an experiment using benchtop instruments to stimulate LEDs and measure photodiodes currents exposed to a range of turbidity calibration solutions in controlled, laboratory conditions (i.e. no variations in ambient light).

Briefly, a Keithley 2400 Source Meter is used to stimulate the LEDs with a constant current of 80 mA, while the photocurrent issued from the photodiodes are measured to a Keithley 2100 Multimeter setup as an Ampere meter. The LEDs excitation current is only briefly maintained during the measurement to avoid detrimental heating effects. The two optical configurations required by the GLI-2 method, i.e. 90° nephelometric (referred also as Active) and 180° attenuation (referred also as Reference) are measured with this setup, and showed Figure 7 for turbidity solutions varying from 0 to 40 NTU. It can be noted that the photocurrents vary as expected: in 90° nephelometric configuration, an increase in turbidity results in an increase of light diffraction and consequently to an increase of the collected light by the active photodiode. In the attenuation configuration, an increase of turbidity leads to an increase of light scattering and absorption, which turns into a decrease of the collected light by the 180° photodiode. A linear relationship between photocurrent and turbidity is observed in all configurations.

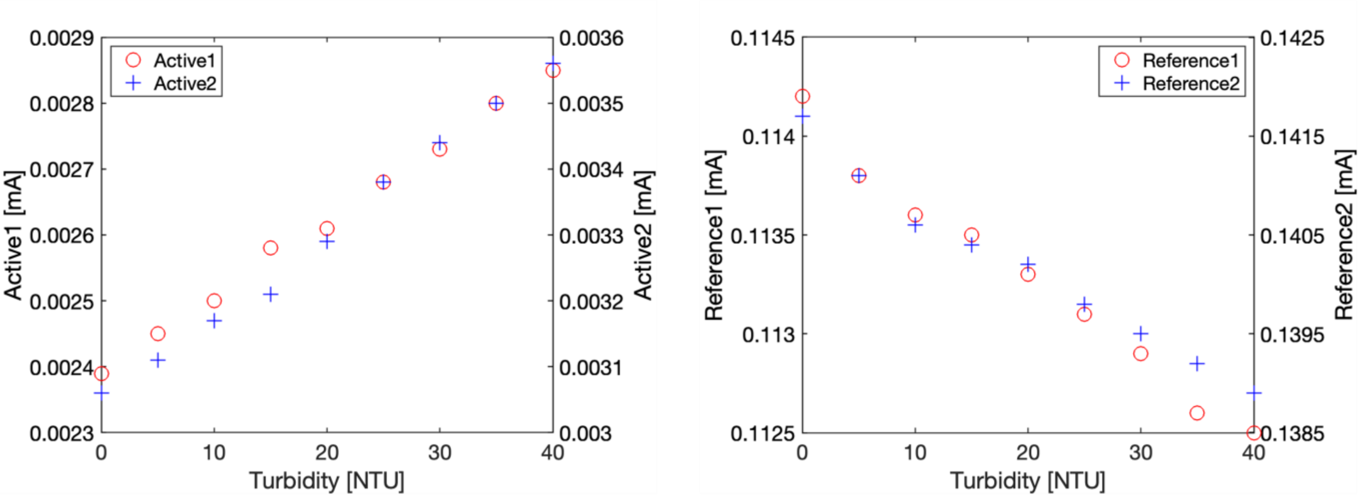


*Figure 7. Photodetector current characterization obtained with benchtop instruments with Formazin solutions ranging from 0 to 40 NTU. Left: 90° nephelometric configuration current for Active1 and Active2 signals. Right: 180° attenuation configuration current for Reference1 and Reference2 signals.*

For both Active and Reference optical configuration, slight discrepancies can be observed, which could be attributed to individual optoelectronic components differences or optical effects due to misalignment or differences in the PDMS transparency. It should be emphasized that the photocurrent variations are rather small, and correspond to approximately 10 nA per NTU in 90° nephelometric configuration, and 40 nA per NTU in 180° attenuation configuration. Thus, the corresponding photocurrent variation to a 0.1 NTU turbidity variation shall be in the range of a nA. Nonetheless, these tests confirms that our sensor design works as expected in the 0 to 40 NTU range.

## *3.2. Sensor calibration*

After this sensor design validation using benchtop instruments, we then replaced the benchtop Source Meter and the Ampere Meter by our custom PCB hosting the ADPD1080 photometric front-end and its additional components. In order to implement ambient light rejection, the excitation light is now modulated and consists in trains of short 3 µs pulses, while scattered/and or absorbed resultant signal is synchronously sampled. Photocurrents generated by the photodiodes are internally amplified by a transimpedance amplifier and conditioned, prior to being converted by a 14-bit ADC, giving an output in counts. In order to translate these counts to turbidity related units, a calibration must be performed for both configuration, 90° nephelometric and 180° attenuation. The settings are optimized for each configuration and are given in Table 2. Nine Formazin turbidity calibration samples are prepared, covering a range from 0 to 40 NTU in 5 NTU increments.

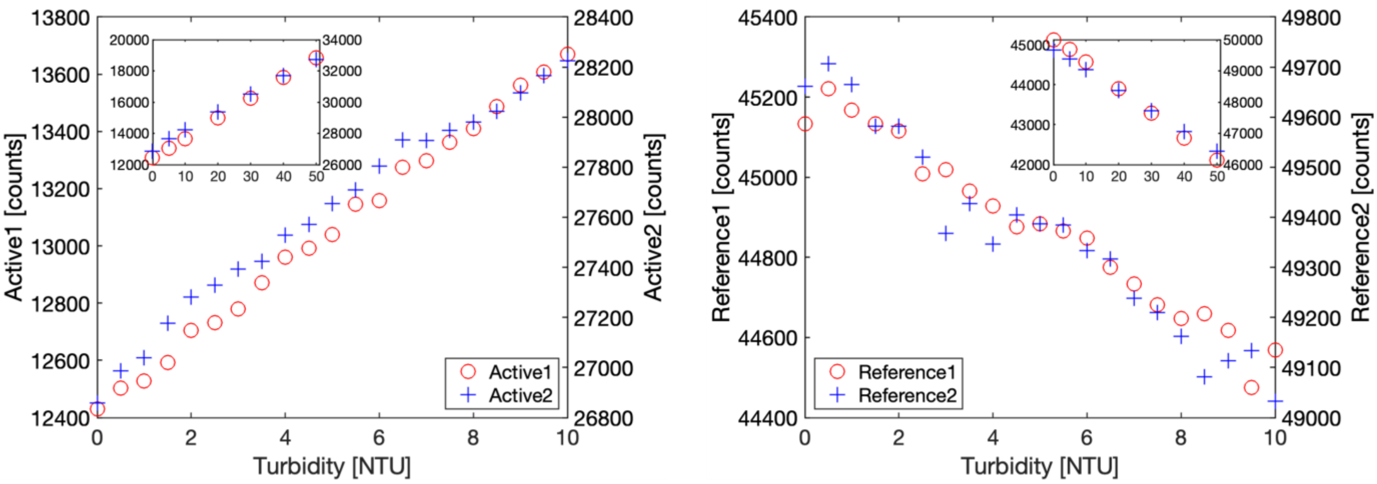


*Figure 8. Calibration experiment with Formazin solutions showing ADC output expressed in counts. Main graphs represent data from 0 to 10 NTU with 0.5 NTU increments, while inset shows the 0 to 50 NTU range. Left: 90° nephelometric configuration ADC counts for Active1 and Active2 signals. Right: 180°attenuation configuration ADC counts for Reference1 and Reference2 signals.*

Figure 8 shows the obtained results in both optical configurations for Active 1, Reference 1, Active 2 and Reference 2 signals. It can be observed that each channel has slightly different characteristics in terms of offset and sensitivity, however both exhibits similar tendencies. In the nephelometric configuration, sensitivity varies from 120 (Active1) to 140 (Active2) counts per NTU approximately, while in the attenuation configuration sensitivity varies from 70 (Reference1) to 80 (Reference2) counts per NTU approximately. However, these differences are not considered as a major issue thanks to the ratiometric nature of the GLI-2 method: in our case, a slightly lower sensitivity is observed on Active1 and Reference1, which means that the photodetector PD1 generates a lower photocurrent than PD2 in the same conditions. As Active1 is in the numerator of equation (2), and Reference1 in the denominator, this difference is cancelled out. This is the same mechanism that gives the GLI-2 some advantages toward biofouling, as if a biofilm partially obstructs an optical port, the sensitivity decrease will be cancelled out by the aforementioned principle. As expected, the 90° nephelometric configuration is more precise and sensitive for the low turbidity range, i.e. 0 to 10 NTU, as the variation in absorption in this range are very small.

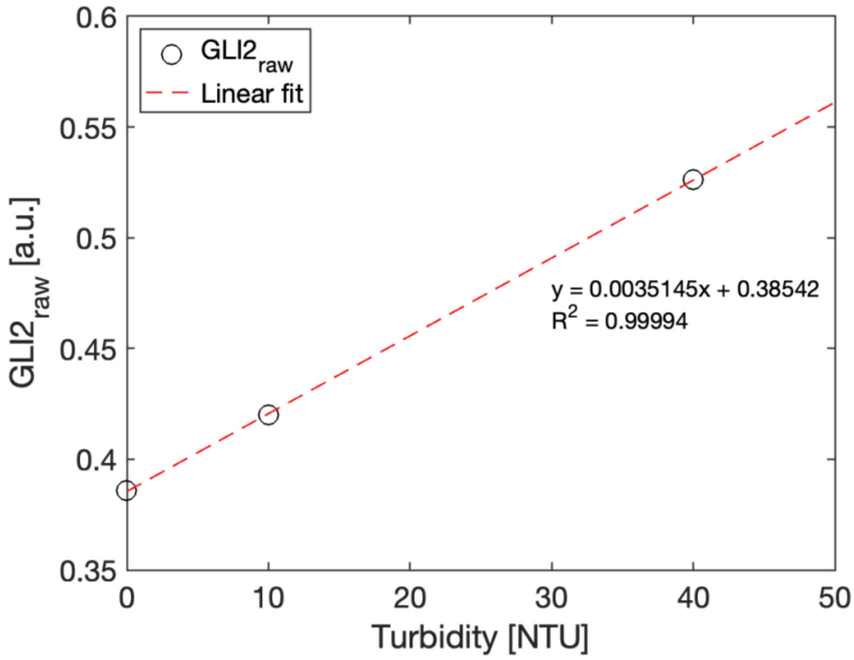


*Figure 9. Three-point calibration of the sensor. $GLI2_{raw}$ values are calculated from the Active1, Active2, Reference1 and Reference2 signals according to equation (1) against three calibration solutions of 0 (deionized water), 10 and 40 NTU (Formazin dilutions).*

A three-point calibration is performed, as recommended by the U.S. Geological Survey for submersible turbidity sensors [38]. The sensor is immersed in three Formazin calibration solutions of 0, 10 and 40 NTU, while the ADC counts for Active1, Reference1, Active2 and Reference2 signals are recorded. The raw GLI-2 output is calculated according to equation (1), and plotted Figure 9.

$$GLI2_{raw} = \sqrt{\frac{Active1*Active2}{Reference1*Reference2}}, \quad (1)$$

From this calibration curve, the calibration coefficients $Cal_{slope}$ and $Cal_0$ are calculated from the linear regression fit of the three-point calibration curve shown Figure 9, to satisfy following equation:

$$GLI2_{NTU} = Cal_{slope}\sqrt{\frac{Active1*Active2}{Reference1*Reference2}} - Cal_0, \quad (2)$$

With the optimized settings from Table 2, the final calibration equation corresponds to the values below:

$$GLI2_{NTU} = 285.714\sqrt{\frac{Active1*Active2}{Reference1*Reference2}} - 110.257, \quad (3)$$

These calibration coefficients are then used to update corresponding variables in the microcontroller code, so the sensor is able to directly output turbidity values in NTU units. Figure 10 shows the results obtained on the 0 to 10 NTU range, with 0.5 NTU increments, and in the extended range of 0 to 50 NTU. Our calibrated GLI2 sensor data is plotted together with a confidence interval of +/- 0.4 NTU around the ideal value, highlighting the good fidelity of the sensor even at these low turbidity values.

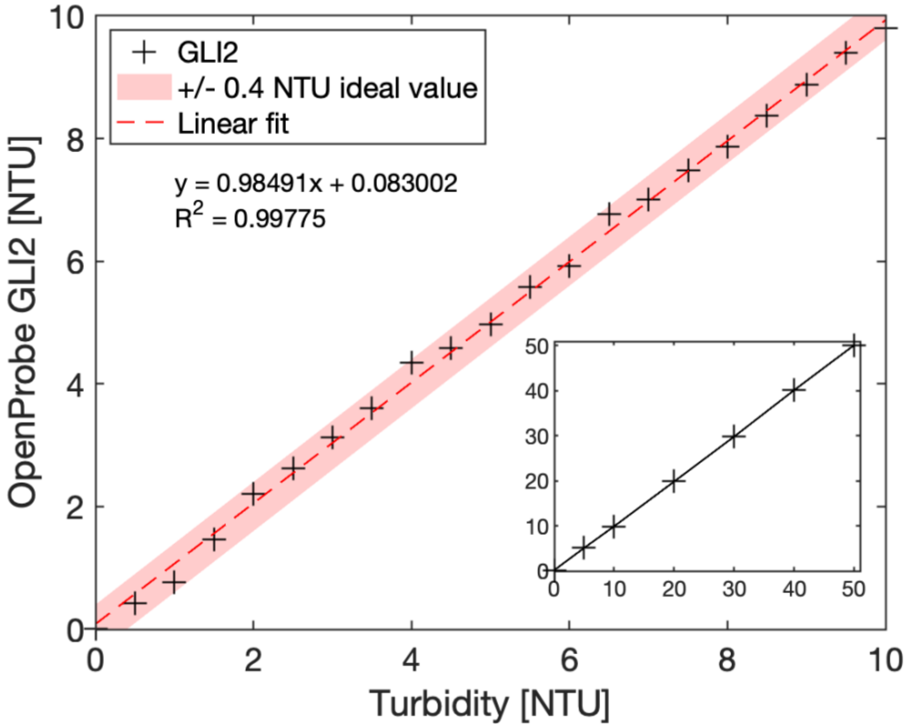


*Figure 10. Calibrated OpenProbe GLi-2 sensor immersed in Formazin calibration solutions from 0 to 10 NTU (main graph), and 0 to 50 NTU (inset). A confidence interval of +/- 0.4 NTU is obtained in the 0 to 10 NTU range.*

While we focused on the 0 to 50 NTU range, good linearity has been observed up to 100 NTU, but due to the large volumes of calibration standard required to fully immerse our sensor, we choose to focus on the lower turbidity range. While we did not perform any testing above 100 NTU, the sensor should also work at higher turbidity values, to the extent that the photometric front-end settings and the calibration curve are optimised for this range, as similar configuration have been successfully used up to 1000 NTU. We finally took the opportunity to compare our sensor implementing the GLI-2 method to the commercial Thermo Fisher Aquafast AQ3010 instrument, the portable handheld device used during our experiments to assess the quality of our Formazin calibration dilutions, that costs approximately 1000 $ USD. The intercomparison plot is given Figure 11.

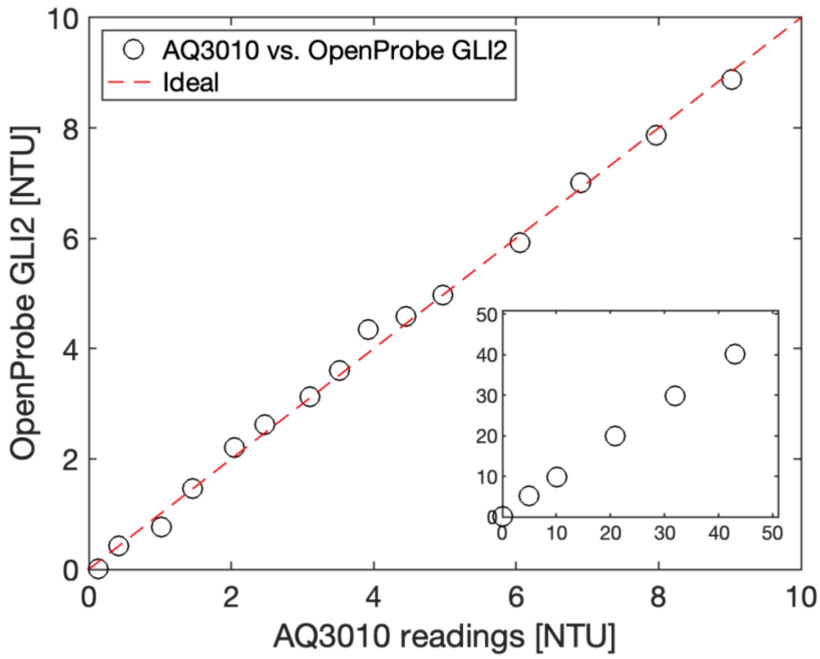


*Figure 11. Intercomparison of our turbidity sensor, OpenProbe GLI-2, versus a portable handheld Thermo Fisher AQ3010.*

The data shows that our sensor compares nicely even in the 0 to 10 NTU range, despite an overall BoM cost of approximately 50 $ USD for a single prototype (excluding the Blue Robotics high-pressure enclosure, which could be replaced by a home-made PVC based enclosure to keep the costs down), with an accuracy of +/-0.4 NTU or better in the 0 to 10 NTU range. While the commercial AQ3010 offers a better accuracy, it is not capable of in-situ measurement, as it requires manual water sampling, followed by pipetting of the sample into a clean vial, as well as a 20 second response time compared to the 100 ms response time of our OpenProbe GLI2 sensor. In terms of cost, the Hydrolab 4-beam turbidity sensor, one of the very few commercial sensors capable of implementing the GLI-2 method in-situ, costs several thousands of dollars.

## 4. Discussion

It is well-know that measuring low turbidity values is particularly challenging. Especially if one considers the additional constraints of an in-situ deployable instrument, as this adds some complexity in the design to make it fully submersible, and some additional issues to handle like ambient light variation, biofouling or temperature variations. Low-cost turbidity sensor development is an active research field, as turbidity is a ubiquitous indicator of water quality, and as such a parameter of interest in many fields, from academic research, to water agencies, or recreational activities like swimming. While many recent studies have shown great developments (as summarised in Table 2), there seems to be currently no low-cost solution for in-situ measurement in the low turbidity range. In this project we thus developed a prototype of a low-cost turbidity meter that is capable of measuring turbidity values in the range of 0 to 50 NTU, with an accuracy of +/- 0.4 NTU after calibration. Compared to a commercial portable handheld instrument, our sensor shows comparable performance at a fraction of the cost. Furthermore, by using a design based on the GLI-2 method, integrating an ambient light-rejection strategy using an integrated photometric front-end, and developing a simple yet effective waterproof enclosure based on SLA 3D printing and PDMS overmolding, this sensor should be capable to be used in-situ in natural waters, as the GLI-2 method offers inherent robustness toward biofouling, LED and photodiode drifts or color effects. Our future works will focus on long-term, field validation of our sensor in water bodies exposed to significant turbidity variations, as well as an intercomparison campaign with a commercial, in-situ GLI-2 sensor in order to further validate these encouraging results.

**Supplementary Materials:** The Arduino code, PCB schematic and layout files in Eagle CAD software format, and the STL files to print the enclosure are available at: https://gitlab.laas.fr/vraimbau/OpenProbe.

**Author Contributions:** Raul Sanchez and Vincent Raimbault contributed to the instrument design, development, prototyping and laboratory testing. Vincent Raimbault, Michel Groc, Renaud Vuillemin and Mireille Pujo-Pay contributed to funding acquisition, supervision and project administration. All authors have read and agreed to the published version of the manuscript.

**Funding:** This work was supported by the CNRS 80|Prime program with the reference OpenProbe. It was partly supported by the French National Program (ANR) ”Investment for Future - Excellency Equipment” project TERRA FORMA with the reference ANR-21-ESRE-0014, It was also partly supported by the LAAS-CNRS micro and nanotechnologies platform (member of the Renatech French national network) and by the MultiFAB project funded by FEDER European Regional Funds and French Région Occitanie under grant agreement number 16007407/MP0011594. Additionnal support was obtained from the Econect project funded by FEDER European Regional Funds and French Région Occitanie under grant agreement number MP00021763.

**Institutional Review Board Statement:** Not applicable.

**Acknowledgments:** The authors would like to thanks Ben Kitchener for giving us some very valuable information on turbidity instruments.

**Conflicts of Interest:** The authors declare no conflict of interest. The funders had no role in the design of the study; in the collection, analyses, or interpretation of data; in the writing of the manuscript; or in the decision to publish the results.

## References

1. Lambrou, T.P.; Panayiotou, C.G.; Anastasiou, C.C. A Low-Cost System for Real Time Monitoring and Assessment of Potable Water Quality at Consumer Sites. In Proceedings of the Proceedings of IEEE Sensors; 2012.
2. Matos, T.; Faria, C.L.; Martins, M.S.; Henriques, R.; Gomes, P.A.; Goncalves, L.M. Development of a Cost-Effective Optical Sensor for Continuous Monitoring of Turbidity and Suspended Particulate Matter in Marine Environment. *Sensors (Switzerland)* **2019**, *19*, 1–21, doi:10.3390/s19204439.
3. Trevathan, J.; Read, W.; Schmidtke, S. Towards the Development of an Affordable and Practical Light Attenuation Turbidity Sensor for Remote near Real-Time Aquatic Monitoring. *Sensors (Switzerland)* **2020**, *20*, doi:10.3390/s20071993.
4. Trevathan, J.; Read, W.; Sattar, A. Implementation and Calibration of an IoT Light Attenuation Turbidity Sensor. *Internet of Things* **2022**, *19*, 100576, doi:https://doi.org/10.1016/j.iot.2022.100576.
5. Sadar, M. *Turbidity Measurement: A Simple, Effective Indicator of Water Quality Change*; 2011;
6. Guo, X.; Stoesser, T.; Zheng, D.; Luo, Q.; Liu, X.; Nian, T. A Methodology to Predict the Run-out Distance of Submarine Landslides. *Comput Geotech* **2023**, *153*, 105073, doi:https://doi.org/10.1016/j.compgeo.2022.105073.

7. Jaijel, R.; Biton, E.; Weinstein, Y.; Ozer, T.; Katz, T. Observations of Turbidity Currents in a Small, Slope-Confined Submarine Canyon in the Eastern Mediterranean Sea. *Earth Planet Sci Lett* **2023**, *604*, 118008, doi:https://doi.org/10.1016/j.epsl.2023.118008.
8. Vousdoukas, M.I.; Aleksiadis, S.; Grenz, C.; Verney, R. Comparisons of Acoustic and Optical Sensors for Suspended Sediment Concentration Measurements under Non-Homogeneous Solutions. In Proceedings of the Journal of Coastal Research; 2011.
9. Pallarès, A.; Schmitt, P.; Uhring, W. Comparison of Time Resolved Optical Turbidity Measurements for Water Monitoring to Standard Real-Time Techniques. *Sensors* **2021**, *21*, doi:10.3390/s21093136.
10. Matos, T.; Faria, C.L.; Martins, M.S.; Henriques, R.; Gomes, P.A.; Goncalves, L.M. Development of a Cost-Effective Optical Sensor for Continuous Monitoring of Turbidity and Suspended Particulate Matter in Marine Environment. *Sensors (Switzerland)* **2019**, *19*, doi:10.3390/s19204439.
11. Omar, A.F. bin; MatJafri, M.Z. bin Turbidimeter Design and Analysis: A Review on Optical Fiber Sensors for the Measurement of Water Turbidity. *Sensors* 2009, *9*.
12. Sadar, M. Turbidimeter Instrument Comparison: Low-Level Sample Measurements - Technical Information Series. *Hach Company. Loveland, CO.* **1999**.
13. Fondriest Environmental Measuring Turbidity, TSS, and Water Clarity Available online: https://www.fondriest.com/environmental-measurements/measurements/measuring-water-quality/turbidity-sensors-meters-and-methods/ (accessed on 2 November 2022).
14. ISO 7027-1 *Water Quality — Determination of Turbidity — Part 1: Quantitative Methods*; 2016;
15. Usepa Method 180.1: Determination of Turbidity by Nephelometry. *ISA Trans* **1993**, *32*.
16. Misaghi, F.; Delgosha, F.; Razzaghmanesh, M.; Myers, B. Guidance Manual for Compliance with the Surface Water Treatment Rules: Turbidity Provisions. *Science of the Total Environment* **2017**, *589*.
17. Epa, U.; of Ground Water, O.; Water, D. *Guidance Manual for Compliance with the Surface Water Treatment Rules: Turbidity Provisions*;
18. Anderson, C.W. *Chapter A6. Section 6.7. Turbidity*; 2005;
19. Kingsbury, F.B.; Clark, C.P.; Williams, G.; Post, A.L. The Rapid Determination of Albumin in Urine. *J Lab Clin Med* **1926**, *11*.
20. Rice, E.W. The Preparation of Formazin Standards for Nephelometry. *Anal Chim Acta* **1976**, *87*, doi:10.1016/S0003-2670(01)83146-9.
21. Kitchener, B.G.B.; Wainwright, J.; Parsons, A.J. A Review of the Principles of Turbidity Measurement. *Prog Phys Geogr* **2017**, *41*, 620–642, doi:10.1177/0309133317726540.
22. Rymszewicz, A.; O'Sullivan, J.J.; Bruen, M.; Turner, J.N.; Lawler, D.M.; Conroy, E.; Kelly-Quinn, M. Measurement Differences between Turbidity Instruments, and Their Implications for Suspended Sediment Concentration and Load Calculations: A Sensor Inter-Comparison Study. *J Environ Manage* **2017**, *199*, 99–108, doi:10.1016/j.jenvman.2017.05.017.
23. Davies-Colley, R.; Hughes, A.O.; Vincent, A.G.; Heubeck, S. Weak Numerical Comparability of ISO-7027-Compliant Nephelometers. Ramifications for Turbidity Measurement Applications. *Hydrol Process* **2021**, *35*, doi:10.1002/hyp.14399.
24. Kitchener, B.G.B.; Dixon, S.D.; Howarth, K.O.; Parsons, A.J.; Wainwright, J.; Bateman, M.D.; Cooper, J.R.; Hargrave, G.K.; Long, E.J.; Hewett, C.J.M. A Low-Cost Bench-Top Research Device for Turbidity Measurement by Radially Distributed Illumination Intensity Sensing at Multiple Wavelengths. *HardwareX* **2019**, *5*, doi:10.1016/j.ohx.2019.e00052.

25. Gantois, F.; Guigues, N.; Raveau, S.; Lepot, B.; Gal, F. *Panorama de l’existant Sur Les Capteurs et Analyseurs En Ligne Pour La Mesure Des Paramètres Physico-Chimiques Dans l’eau*; 2016;
26. Fay, C.D.; Nattestad, A. Advances in Optical Based Turbidity Sensing Using Led Photometry (Pedd). *Sensors* **2022**, *22*, doi:10.3390/s22010254.
27. Gillett, D.; Marchiori, A. A Low-Cost Continuous Turbidity Monitor. *Sensors (Switzerland)* **2019**, *19*, doi:10.3390/s19143039.
28. Trevathan, J.; Read, W.; Schmidtke, S. Towards the Development of an Affordable and Practical Light Attenuation Turbidity Sensor for Remote near Real-Time Aquatic Monitoring. *Sensors (Switzerland)* **2020**, *20*, doi:10.3390/s20071993.
29. Zang, Z.; Qiu, X.; Guan, Y.; Zhang, E.; Liu, Q.; He, X.; Guo, G.; Li, C.; Yang, M. A Novel Low-Cost Turbidity Sensor for in-Situ Extraction in TCM Using Spectral Components of Transmitted and Scattered Light. *Measurement (Lond)* **2020**, *160*, doi:10.1016/j.measurement.2020.107838.
30. Metzger, M.; Konrad, A.; Blendinger, F.; Modler, A.; Meixner, A.J.; Bucher, V.; Brecht, M. Low-Cost GRIN-Lens-Based Nephelometric Turbidity Sensing in the Range of 0.1–1000 NTU. *Sensors (Switzerland)* **2018**, *18*, doi:10.3390/s18041115.
31. Parra, L.; Rocher, J.; Escrivá, J.; Lloret, J. Design and Development of Low Cost Smart Turbidity Sensor for Water Quality Monitoring in Fish Farms. *Aquac Eng* **2018**, *81*, 10–18, doi:10.1016/j.aquaeng.2018.01.004.
32. Kelley, C.D.; Krolick, A.; Brunner, L.; Burklund, A.; Kahn, D.; Ball, W.P.; Weber-Shirk, M. An Affordable Open-Source Turbidimeter. *Sensors (Switzerland)* **2014**, *14*, 7142–7155, doi:10.3390/s140407142.
33. Hydrolab OTT Technical White Paper - 4-Beam Turbidity.
34. Nguyen, B.; Goto, B.; Selker, J.S.; Udell, C. Hypnos Board: A Low-Cost All-in-One Solution for Environment Sensor Power Management, Data Storage, and Task Scheduling. *HardwareX* **2021**, *10*, doi:10.1016/j.ohx.2021.e00213.
35. Thaler, A.; Sturdivant, K.; Neches, R.; Black, I. *OpenCTD Construction and Operation*;
36. Venzac, B.; Deng, S.; Mahmoud, Z.; Lenferink, A.; Costa, A.; Bray, F.; Otto, C.; Rolando, C.; le Gac, S. PDMS Curing Inhibition on 3D-Printed Molds: Why? Also, How to Avoid It? *Anal Chem* **2021**, *93*, 7180–7187, doi:10.1021/acs.analchem.0c04944.
37. Nightingale, A.M.; Hassan, S.U.; Warren, B.M.; Makris, K.; Evans, G.W.H.; Papadopoulou, E.; Coleman, S.; Niu, X. A Droplet Microfluidic-Based Sensor for Simultaneous in Situ Monitoring of Nitrate and Nitrite in Natural Waters. *Environ Sci Technol* **2019**, *53*, 9677–9685, doi:10.1021/acs.est.9b01032.
38. Anderson, C.W.; Survey, U.S.G. *Chapter A6. Section 6.7. Turbidity*; Version 2.1.; Reston, VA, 2005;